J Therm Anal Calorim (2017) 128:1327–1334
DOI 10.1007/s10973-016-6075-5

Preparation and physicochemical characterization of binary composites palygorskite–chitosan for drug delivery

Ana Cristina Sousa Gramoza Vilarinho Santana[1] · José Lamartine Soares Sobrinho[2] · Edson Cavalcanti da Silva Filho[3] · Lívio Cesar Cunha Nunes[2]

Received: 18 May 2016 / Accepted: 19 December 2016 / Published online: 4 January 2017

Abstract This work aimed the evaluation of pH influence in the obtainment of composites from palygorskite (PAL) and chitosan (CS). The materials PAL/CS-1 and PAL/CS-2 were obtained by similar methodology with modified pHs: 5.0 ± 0.5 and 11.0 ± 0.5, respectively. Both materials were evaluated for specific surface area analysis, elemental analysis, XRD, FTIR, thermal analysis, MEV and interaction drug composite, using 5-aminosalicylic acid (5-ASA) as model. The surface area analysis data showed the reduction in PAL/CS-2 related to CS presence on surface in contrast with PAL/CS-1, which corroborate with elemental analysis present nine times more of CS in PAL/CS-2 composition. Regarding to XRD data, the interaction of CS with PAL did not cause modification in clay structure in PAL/CS-2. These results were confirmed by FTIR data with the N–H deformation vibration in PAL/CS-2 while PAL/CS-1 was invariable to PAL. In thermal analysis, results were observed 60.2% residual mass to PAL/CS-2, which it was lower than PAL (87.2%) and PAL/CS-1 (86.7%), due to CS decomposition which had enthalpy energy of 62.1 J g^{-1} K^{-1}, confirming the data previously cited. PAL/CS-2 presented 5-ASA adsorption of 7.9 mg g^{-1}, which was inferior to others probably caused by scarcity of active sites of PAL already occupied by CS. These results showed that pH control was fundamental to enhance efficiency of obtainment of composite in basic pH because the decrease in CS protonation degree increasing interaction between this one and PAL, although it contributed to decrease in 5-ASA adsorption due to low availability of interaction sites.

Keywords 5-ASA · Mesalazine · Adsorption · Composite

Introduction

Materials organics or inorganic are commonly used in their pure form but oftentimes do not meet the desired properties. Organic–inorganic composites have attracted considerable attentions in the past decades because the incorporation of inorganic filler into polymer matrix brings surprising hybrid performance superior to their individual components. They are able to generate benefits as high hardness, increase resistance and enhance barrier properties which depend of compounds composition, properties and structure and interfacial interaction. These materials offer numerous applications in biotechnology field. Among inorganic compounds, the clays have been used in industrial area to enzyme immobilization, chromatographic area, oil clarification, removal of inks as well as cosmetic and pharmaceutical area [1–4].

Among clay minerals used in biotechnology field, there is palygorskite (PAL), also known as Attapulgite, fibrous clay formed from two inversed silica tetrahedral sheets and a magnesium octahedral sheet between them, characterized as 2:1 layer phyllosilicate. Due to its porous structure generated by arrangement of layers, the PAL has been know by high surface area. Its negative charge, between pH

✉ Ana Cristina Sousa Gramoza Vilarinho Santana
acsgv@hotmail.com

[1] Department of Pharmaceutical Sciences, Federal University of Pernambuco, Av. Professor Moraes Rego 1235, Recife, Pernambuco 50670-901, Brazil

[2] Department of Chemistry, Federal University of Piaui, Ministro Petrônio Portela Campus, Teresina, Piauí 64049-550, Brazil

[3] Department of Pharmacy, Federal University of Piaui, Ministro Petrônio Portela Campus, Teresina, Piauí 64049-550, Brazil

2.0 up to 11.0, allows the electrostatical interaction with cations besides having moderate capacity cationic change which offers to PAL great mechanical properties favoring interactions of clay with a great number of organic and inorganic constituents. In related to organic compounds, polymers or copolymers as poly(vinyl alcohol) (PVA), polyethylene, polyimide and chitosan (CS) has been studied to development of new composite in order to obtain properties as increase of metals carrier, thermal stability, higher mechanical strength, toughness of the matrix and drug delivery. The interaction between both materials occurs by hydrogen bonds through reactive silanol groups (Si–OH) on the surface clay, [1, 5–9].

CS is a cationic copolymer biocompatible, biodegradable and nontoxic compound of glucosamine and *N*-acetylglucosamine units and widely used as adsorbent in several areas such as contaminant adsorption and loading drugs. Although CS had great adsorptive capacity to anionic compounds, its mechanical strength is weak and is easily dissolved in strong acid solution, which cause drawback to its utilization as adsorbent. To achieve desirable functions, some inorganic compound has been incorporated into CS by various techniques. Therefore, the use of PAL particles to immobilization of CS can enhance the adsorption of the copolymer in unfavorable conditions. The presence of reactive amino ($–NH_3^+$) and hydroxyl (–OH) groups becomes the CS able to possible interactions with reactive sites of clay which improve its mechanical properties and resistance to water [1, 9–11].

In this way, composites formed by PAL and CS generate synergic effect with improvement of physicochemical as well as drug delivery properties adding advances to pharmaceutical area. So, this study aimed the development of composite from PAL and CS biomaterials using different pH once this parameter has fundamental importance in the interaction of both. As model drug was used the 5-aminosalicylic acid (5-ASA), potent anti-inflammatory drug used to Chron's disease and ulcerative colitis. It has solubility in pH less than 2 or more than 5.5 and pKa 6.0 showing a protonated amine ($–NH_3^+$) [12].

Materials and methods

Materials

Chitosan (CS) powder was acquired from Polymar Ltda with 86.2% deacetylation degree. Palygorskite (PAL) was acquired by Mineração Coimbra Ltda, Guadalupe-PI (Brazil). 5-Aminosalicylic acid (5-ASA) was purchased from Pharmanostra Company. Sodium hypochlorite (3.6 mass%), hydrogen peroxide (35 mass%) and glacial acetic acid were used with analytical grade.

Deodorization of CS

CS suspension was prepared with purified water, and sodium hypochlorite 3.6 mass% was added for reducing crab or shrimṕs characteristic odor, under magnetic stirring for 1 h, at 298 K [13]. The aim was to reduce the odor and remove residual pigments, which may interfere under desired interactions. CS was isolated by centrifugation at 3000 rpm for 5 min, washed until neutral pH, and the powder was dried at 353 K for 4 h.

Treatment of PAL

Two hundred grams of PAL *in natura* was washed with purified water and dried for two days at 303 K. PAL was dispersed in 400 mL of sodium acetate buffer solution pH 5.0 ± 0.5 under magnetic stirring until temperature stabilization at 323 K, and 150 mL of hydrogen peroxide was added in other to withdraw organic materials inside of pores. The system was maintained as long as any reaction (foaming) was observed [14]. PAL suspension was isolated by centrifugation at 3000 rpm for 5 min, washed with purified water, dried and sieved at 200 mesh.

Obtainment of PAL/CS (1:1)

PAL/CS-1 was prepared according to Dader et al. [15] by solubilization of the 2 g CS in acetic acid solution (1 mass%), under magnetic stirring for 4 h. The pH of solution was adjusted to 5.0 ± 0.5 with NaOH 1.0 mol L^{-1}. Two gram of PAL suspension was prepared in purified water under magnetic agitation for 4 h. Then, CS solution was added slowly to PAL suspension at 323 K stirring for 48 h. The pH was controlled until finish of reaction. After the mixture was centrifuged at 4000 rpm for 5 min, washed in order to withdraw all the residual acetate, dried at 333 K for 24 h and sieved at 200 mesh.

This methodology also was carried out to obtain the material PAL/CS-2. However, in the end, the process the pH was increase to 11.0 ± 0.5. This material was obtained by coprecipitation.

Interaction drug–material

The adsorption of materials for 5-ASA was carried out by employing of 500 mg of PAL, CS and PAL/CS to 100 mL 5-ASA solution of 1,0 mg mL^{-1} with phosphate buffer pH 6.8 ± 0.1 under stirring at 130 rpm and at 303 K for 48 h (incubator Shaker SL222) obtainment the proportion 1:2 (material/drug) to each system [2, 10]. The high concentration of 5-ASA was used to obtain the maximum adsorption of drug by materials. The pH 6.8 was used due to solubility of CS at acid pH which would prevent the

evaluate of drug adsorption on copolymer. After adsorption, the samples was centrifuged at 4000 rpm for 3 min and the supernatant solution concentration was measured using a UV–Vis spectrophotometer at 330 nm, it determined by scanning and calibration curve analysis ($r^2 = 0.9994$). The reverse calculation was performed to determine the drug portion adsorbed by materials. The encapsulation efficiency (EE) was calculated by the equation as follows:

$$\mathrm{EE}\,(\%) = \frac{\mathrm{mo} - \mathrm{mi}}{\mathrm{mo}} \times 100 \quad (1)$$

where mo and mi the 5-ASA mass in the medium before and after adsorption by materials, respectively [16].

Characterization

Surface area, diameter and pore volume were calculated to Brunauer–Emmett–Taller (BET) and Barret–Joyner–Halenda (BET/BJH) procedure by ASAP 2420 equipment, V2.02. The samples were heated to 523 K for 2 h before analysis.

The carbon, hydrogen and nitrogen contents in the CS were determined through elemental analysis on a PerkinElmer CHN 2400, using Pregl–Dumas method. The combustion of samples was pure oxygen atmosphere, and gases were quantified in detector thermal conductivity detector.

X-ray diffraction (XRD) was carried out on Shimadzu® diffractometer, model XRD 6000, with Cu-$K\alpha$ radiation. Diffractograms were scanned in a scattering range from 5 to 50° (2θ) with resolution of 0.02° and scanning speed of 1.2° min^{-1}, applying an accelerating voltage of 40 kV, and a current intensity of 30 mA.

Fourier transform infrared spectroscopy (FTIR) spectra were recorded in the 4000–400 cm^{-1} spectral region performed on Agilent, Cary 630 FTIR.

The differential scanning calorimetry (DSC) and thermogravimetric analysis (TG) were taken by SDT Q600V 20.9 instrument, under nitrogen atmosphere. The system was calibrated with zinc and calcium oxalate monohydrate to DSC and TG analysis, respectively. About 5 mg of the samples was placed in aluminum pan and heated from room temperature to 1273 K, at a heating rate of 283 K min^{-1} and using a synthetic air flow of 100 mL min^{-1}.

Scanning electron microscopy (SEM) images were obtained by using FEI, QUANTA FEG 250®. The samples were conditioned by gold covering for 15 min. Photomicrographs were captured at 5.00 kV with a magnification of 5000×.

Results and discussion

The surface analysis is among the parameters most important to evaluate the retention capacity and interaction of the adsorbent [17]. In S_{BET} (Table 1), showed the decrease in specific surface area of PAL/CS-1 (13.49%) and mainly of PAL/CS-2 (56.92%) what indicate the occurrence preferential of electrostatic interactions and may be also mediated by intermolecular hydrogen bonding between amino ($-NH_3^+$) and hydroxyl (–OH) groups present in CS and silanol ($\equiv$Si–OH) groups in PAL. This reduction occurs due to the presence of CS macromolecular chain, which might block the exiting pores hindering N_2 intrusion. Furthermore, the interaction might generate flocculation which greatly reduced specific surface area [18–20]. According to IUPAC recommendation, all the materials consisted of mesopores ($2 < d < 50$ nm).

Table 1 Surface of materials PAL, PAL/CS-1 and PAL/CS-2

Materials	$S^{a}_{\mathrm{BET}}/\mathrm{m}^2\ \mathrm{g}^{-1}$	$S^{b}_{\mathrm{ext}}/\mathrm{m}\ \mathrm{g}^{-1}$	$V^{c}_{\mathrm{total}}/\mathrm{cm}^3\ \mathrm{g}^{-1}$	d^{d}/nm
PAL	118.04	146.71	0.34	11.62
PAL/CS-1	102.12	138.28	0.33	12.92
PAL/CS-2	50.85	86.51	0.12	93.16

[a] Specific surface area, [b] external surface area, [c] total pore volume, [d] average pore diameter

S_{ext}, Table 1, is related to defects on PAL particle surface in the grooves and fissures forms of small depth, and there is decrease of 41.03% in PAL/CS-2 compared to PAL/CS-1 (5.75%) suggesting that the interaction reflected in morphology particle surface with characteristics less fibrous as showed by PAL [7, 21]. Regarding to V_{total}, there is a reduction of 2.94% in PAL/CS-1 and of 64.71% in PAL/CS-2 what confirm the occupation pore volume in this one.

In Table 2 were described the elemental analysis data of materials CS, PAL/CS-1 and PAL/CS-2.

PAL/CS-2 obtained 2.13 and 17.99 mmol g^{-1} of nitrogen and carbon, respectively, by elemental analysis (Table 2). Since CS has 1N:6, 1N:5O and 1N:9H it indicates the existence of 2.98% N, 17.99% C, 17.04% O and 3.96% H and totalizing 41.97% in CS mass present in the PAL/CS-2 once atoms carbon and nitrogen are present only in copolymer evidencing composite formation. To PAL/CS-1, the amount of CS loaded in its composition was 2.71 mmol g^{-1} (3.25%) C, 0.24 mmol g^{-1} (0.33%) N, 1.2 mmol g^{-1} (1.92%) O and 2.16 mmol g^{-1} (0.22%) H. This reflected the low interaction between PAL and CS with 5.72% this one. These data corroborate with specific surface area analysis.

The exchange of solution pH was important factor to obtain of composite. The increase pH of 5.0–11.0 provided was able to elevate about nine times the amount of CS adsorbed on PAL/CS-2 compared to PAL/CS-1. This can be explain because at pH 5.0 the CS has a greater protonation degree, with amino groups pKa about 6.5, being

Table 2 Elemental analysis of carbon (C), hydrogen (H) and nitrogen (N) of CS, PAL/CS-1 and PAL/CS-2

Materials	%C	%H	%N	C/mmol g^{-1}	H/mmol g^{-1}	N/mmol g^{-1}
CS	38.98	7.00	6.73	32.48	70.00	4.80
PAL/CS-1	3.25	1.96	0.33	2.71	19.60	0.24
PAL/CS-2	17.99	3.96	2.98	14.99	39.60	2.13

necessary a small quantity of CS to equalize the negative charge of PAL. Besides, acid pH provided large amount of H^+ ions free in solution what created a competition between ones and CS protonated that can difficult the interaction of the copolymer with PAL [18, 22, 23]. At pH 11.0, the obtainment of composite was more efficient due to increase at pH led to decrease in protonation degree raising the necessary amount to equalize the negative charge of silicate which enhanced the quantity of CS absorbed.

These results were different to presented by Dader et al. [15], who used the CS in its maximum protonation (pH 5.0) as adsorbate and clay montmorillonite (MMT) as adsorbent. This is attributed to hardness of fibrous clay PAL that unlike MMT of lamellar structure, it does not suffer expansion in its basal layers [20].

Figure 1 shows the XRD spectra the crystalline state of materials. In Fig. 1a, the partial crystallinity of CS was evidenced by two characteristic peaks one at 9.8° and the other at 20.2° due to due to strong intra- and intermolecular hydrogen bonding, in accordance with Huang et al. [1]. With respect to PAL, Fig. 1b, one can note the presence of crystalline peaks characteristic of clay at 8.6°, 13.9°, 16.3°, 19.8° and at 28.9° [5, 24].

To analyze Fig. 1c, d, the materials obtained presents well defined peaks PAL. PAL/CS-1 has similarity with clay without peaks of CS. In PAL/CS-2 is noted a reduction of crystallinity compared to PAL. From peak, integrate was possibly observed in the peak area between 12° and 30° of 806.3 to PAL, while to PAL/CS-2 was 1059.6 showing the increase in area by peak broadening due to decrease in crystallization because of the presence of CS. Thus, it suggests the occurrence of inclusion of copolymer inside the pores of fibrous clay but with advantage on surface due to invariability of shift of peaks positions without modifications in clay structure. Moreover, the fibrous structure (three dimensional) of PAL which did not expansion of the basal layers as occurrence with lamellar crystalline silicates [19, 20, 25].

The FTIR spectra are evidenced in Fig. 2. The data exhibited in Fig. 2a showed CS the larger absorption bands were: 3358 cm^{-1} (strong stretching related to O–H and N–H vibration); 2917 and 2875 cm^{-1} (C–H stretching); 1646 and 1579 cm^{-1} (N–H deformation); 1419 and 1319 cm^{-1} (C–O stretching), 1378 cm^{-1} (C–N stretching); and 1060 and 1027 cm^{-1} (C–O skeleton vibration) [26].

The positions that presented more prominent bands related to PAL, Fig. 2b, were: 3614 cm^{-1} (Al_2–OH

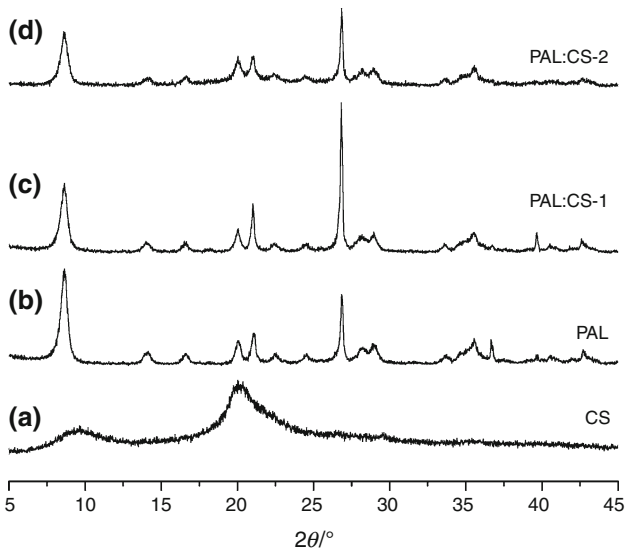

Fig. 1 XRD of CS (*a*), PAL (*b*), PAL/CS-1 (*c*) and PAL/CS-2 (*d*)

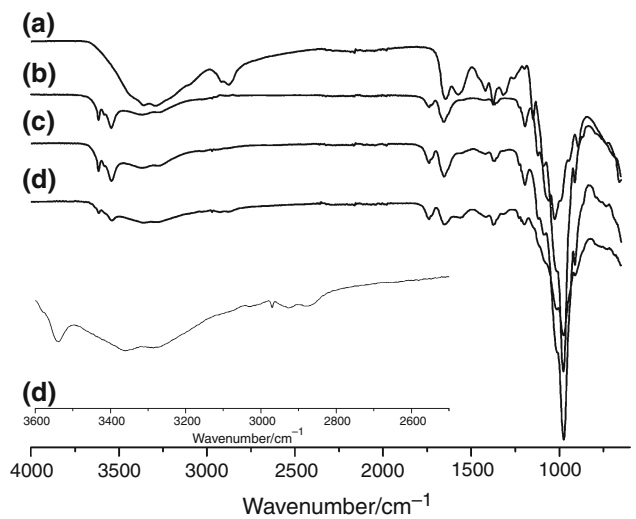

Fig. 2 FTIR spectrum of CS (*a*), PAL (*b*), PAL/CS-1 (*c*) and PAL/CS-2 (*d*)

stretching and Al/Fe–OH); 3582 cm^{-1} (stretching of adsorbed water molecules forming Al–Fe_3^+–OH); 3543 cm^{-1} (strong stretching related to coordinated water forming Al/Mg–OH, Fe/Mg–OH and Fe_2–OH); 1655 cm^{-1} (deformation of adsorbed and coordinated water); and the vibration between 1193 to 977 cm^{-1}, linked to Si–O–Si which is stronger due to the formation of O–SiO_3 [27–29].

In Fig. 2c, it is observed that PAL/CS-1 was similar to PAL what suggest the absence of interaction between PAL and CS, in contrast with PAL/CS-2, Fig. 2d. PAL/CS-2 exhibited bands in 3613 and 3539 cm^{-1} (stretching of O–H) and 1198, 1015, 977 and 911 cm^{-1} (characteristic bands silicate) similar to PAL. However, there was the reducing these bands, which reflected the effect of CS onto the surface PAL. Besides PAL/CS-2 showed bands in 2928 and 2876 cm^{-1} (stretching of C–H), 1649 and 1563 cm^{-1} (deformation of N–H), 1419 and 1319 cm^{-1} (stretching of C–O) and 1375 cm^{-1} (stretching of C–N) similar to CS. The shift of N–H band probably is due to the deformation vibration of the protonated amino group (–NH_3^+) of CS [19]. This analysis has been agreement with XRD data, elemental analysis and surface area analysis indicating the immobilization of CS onto the surface of PAL in PAL/CS-2.

Figure 3 exhibits TG/DTG and DSC data to analyze the events generate by increase in temperature. In Fig. 3a, e, CS presents 8.9% mass loss between 310 and 423 K with maxima of 332 K in DTG curve related to elevate water retention capacity of copolymer with enthalpy associated with 244.6 J g^{-1} K^{-1}, similar to Darder and Ruiz-Hitzky [15]. The second event in TG curve was between 473 and 673 K with maxima of 566 K in DTG curve, showed 58.8% mass loss involving decomposition of the CS with energy of 145.9 J g^{-1} K^{-1} due to high temperatures [2, 19]. The residual mass loss was of 32.2%.

As reported by Yan et al. [30] and Oliveira et al. [31], PAL present three steps of mass loss, Fig. 3b, e. The step of water loss occurs in the 303–403 K range with maxima of 343 K in DTG curve correspondent to mass loss of 6.1% and is related to partial loss of water molecules in the interlayer cations of PAL, also knowledge as zeolitic water involving enthalpy energy of 203.5 J g^{-1} K^{-1}. The second step was between 389 and 506 K, which showed maxima of 459 K in DTG curve, there occurred evaporation of residual mass of zeolitic water with a loss of 2.5% and energy of 12.3 J g^{-1} K^{-1}. In the range of 568–833 K, there was the mass loss related to structural (or coordinated) water and to dehydroxylation associated with octahedral sheets of PAL with a loss of 4.1% with 13.2 J g^{-1} K^{-1} of enthalpy energy [19, 30].

PAL/CS-1, Fig. 3c, e, showing three events at 313–373, 398–498 and 500–883 K similar to PAL where the second first are related to partial (4.6%) and residual (2.2%) loss of zeolitic water, respectively, and the third was due to loss of structural water and dehydroxylation of clay minerals with loss of 6.5% in mass. The DTG curve in the last one range was viewed as two events: one at 613 K and another at 838 K. According Oliveira et al. [31], this can occur due to elimination of OH ions in the form of water vapor causing in the sample a partial distribution of the crystal structure by rearrangement of atoms which required a total energy of 14.4 J g^{-1} K^{-1}, slightly larger than PAL due to the interaction, even low, occurred with CS. Besides this, by analyzing residual it infers that can be compose almost entirely for clay with 86.7% final mass compared to PAL with 87.2%. The results corroborate with the others analysis, which evidenced low amount of chitosan adsorbed on material.

Between 303 and 388 K the PAL/CS-2 presented two main events (Fig. 3d, e). One refers to loss of 9.8% related to evaporation of adsorbed water molecules and the second in 477–873 K range occurred organic material decomposition with mass loss of 28%, with peaks in 323 and 556 K in DTG curve, respectively, similar to CS (Fig. 3d). These enthalpy energy associated with events were 324 J g^{-1} K^{-1}, spending more energy to evaporation of trapped water, and 62.1 J g^{-1} K^{-1}, respectively.

Two others events are better perceived in DTG curve (Fig. 3d, e). One between 413 and 503 K with a maximum of DTG curve in 460 K the mass loss of 2.4%, corresponds to loss of zeolitic residual water involving 10.7 J g^{-1} K^{-1}, as PAL. Another step was observed in 673–773 K range had maximum of 708 K in DTG curve, which was due to decomposition of OH ions of PAL with enthalpy energy associated with 6.5 J g^{-1} K^{-1} [31]. The residual mass of PAL/CS-2 was lower than PAL with 60.2% of mass suggesting the coated of the PAL by CS, as evidenced by elemental and specific surface area analysis which about 41% of CS was present in material.

Figure 4 can be observed the morphology of materials by scanning electronic microscopic analysis.

The CS structure is compact and smooth, Fig. 4a, compared to fibrous morphology and elongated of PAL, similar to needles and rods due to hexagonal structure, Fig. 4b [7]. In Fig. 4c, PAL/CS-1 presents structure fibrous similar to parent clay due to low amount of CS adsorbed on PAL surface. However, PAL/CS-2, Fig. 4d, shows morphology compacted and lower amount crystals on surface which were less than 5 μm unlike PAL and PAL/CS-1. Therefore, this analysis evidenced the insertion of CS on PAL structure what corroborate with XRD data and BET with morphology modified by occlusion of pores and decrease in specific surface area confirming the interaction between both causing the coverage on PAL surface.

Figure 5 shows the encapsulation efficient (EE) of 5-ASA adsorbed by materials.

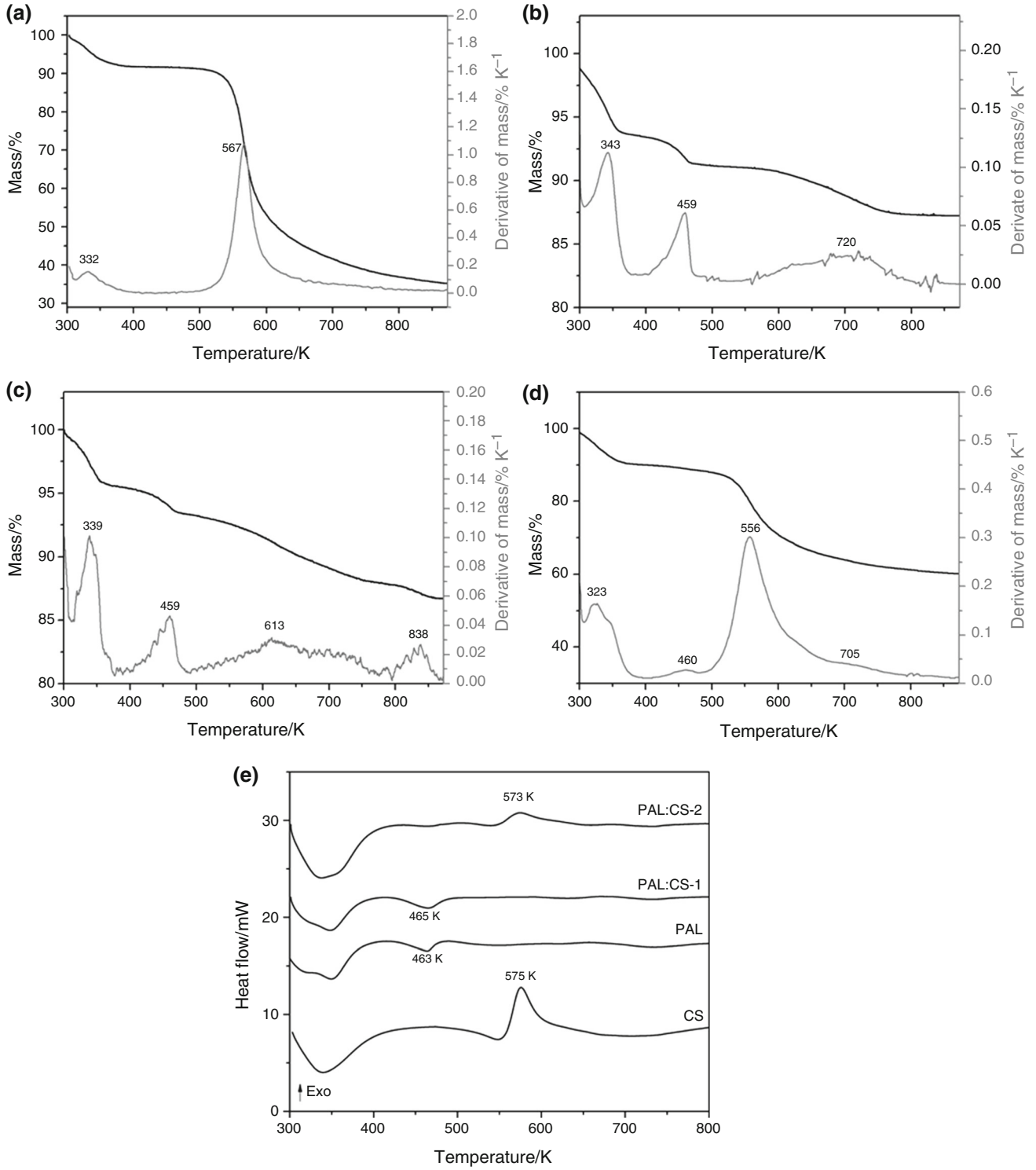

Fig. 3 TG/DTG data of CS (**a**), PAL (**b**), PAL/CS-1 (**c**) and PAL/CS-2 (**d**)

To analyzing PAL/CS-1, it is noted that 17.3 mg of 5-ASA was adsorbed per gram of material, similar to PAL with 19.3 mg g^{-1}, Fig. 5. These data did not exhibit significant difference between both what corroborate with previously analysis mentioned proving the low amount of CS present in this material which did not possible the composite formation. Therefore, the actives sites charged of clay were available to interact with 5-ASA as opposite to PAL/CS-2.

The data confirm the great complexation of CS with EE of 26.99 mg g^{-1} of drug adsorbed. This result was

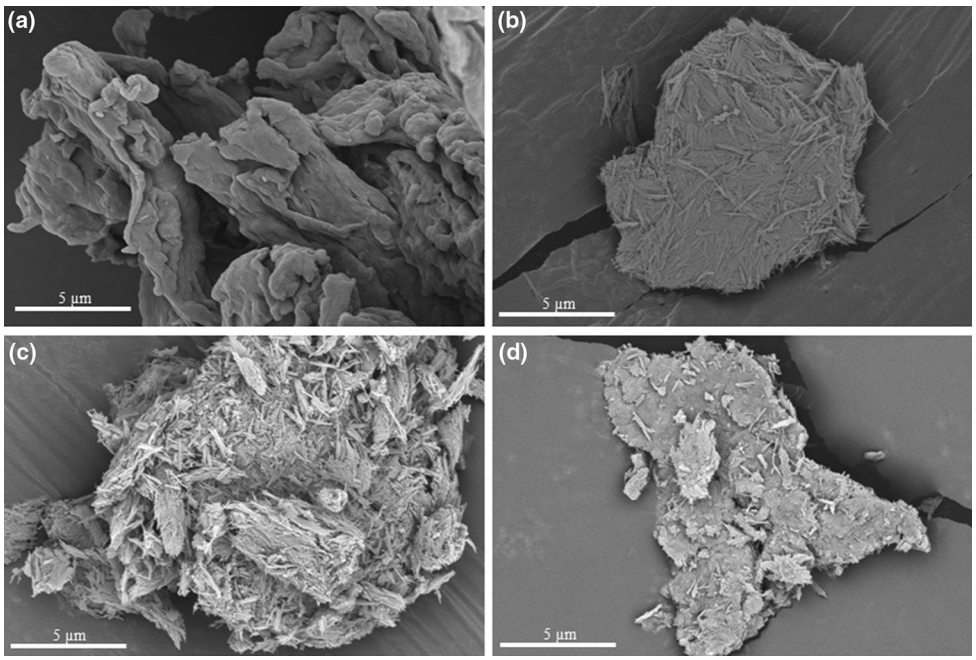

Fig. 4 SEM images of CS (**a**), PAL (**b**), PAL/CS-1 (**c**) and PAL/CS-2 (**d**)

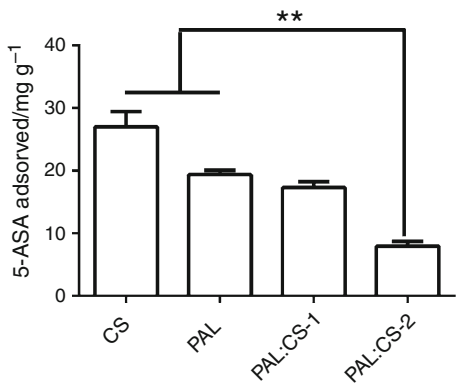

Fig. 5 Encapsulation efficient of 5-ASA adsorbed on CS, PAL, PAL/CS-1 and PAL/CS-2. Difference between materials was determined by variance analysis, one-way ANOVA, followed by Newman–Keuls as posttest ($n = 3$, $^{**}p < 0.05$)

mediated by no covalent interaction as hydrogen bonds between reactive carboxyl, hydroxyl and amino groups of 5-ASA and hydroxyl and amino present in free polysaccharide [32].

The PAL/CS-2 displayed adsorption ratio of 7.9 mg of 5-ASA per gram of material. Although occurred of composite formation in PAL/CS-2, as observed for the thermal properties and physicochemical properties, it led to decrease in drug adsorption when compared to CS and PAL alone, Fig. 5. The reduction of adsorptive capacity of PAL/CS-2 can associate with interaction between active groups of copolymer, amino ($–NH_3^+$) and hydroxyl (–OH), and metallic cations and silanol group (–SiOH) of clay mineral. Thus, it suggest the reduction of available active sites on material to interact with drug once 5-ASA has groups similar to CS. Moreover, the formation of uncharged complex may be the main reason for 5-ASA sorption reduction [8] since the low protonation of CS favored the attractive forces leading to its flocculation in pH > 6.7, as evidenced also by An and Dultz [18]. This way the aggregation caused by coprecipitation technique difficulted the interaction between active sites of drug and materials.

Conclusions

This study revealed the composite formation from chitosan and palygorskite with efficiency by coprecipitation technique using basic pH unlike of showed in the literature but with other kind of clay. Therefore, the fundamental importance of pH control since the protonation degree of CS was crucial to development of composite.

The amount of CS coprecipitated under PAL surface was about 41% causing the occlusion of pores of clay, which reduced its specific surface area with noteworthy morphology changes. These modifications were observed yet by FTIR with interactions between reactive groups of both materials, by XRD with reduction of crystallinity and by thermal analysis that presented considerable loss mass events in composite formed PAL/CS-2.

Despite of data observed, the composite PAL/CS-2 contributed of negative way to drug adsorption. It is suggested that this fact occurred by flocculation of CS, which contributed to unavailability active sites to bind with the drug and formation of uncharged complex.

Acknowledgements CNPq, LAPCOM-UFPI, LIMAV-UFPI and NCQMC-UFPE.

References

1. Huang D, Wang W, Xu J, Wang A. Mechanical and water resistance properties of chitosan/poly(vinyl alcohol) films reinforced with attapulgite dispersed by high-pressure homogenization. Chem Eng J. 2012;210:166–72.
2. Aguzzi C, Capra P, Bonferoni C, Cerezo P, Salcedo I, Sánchez R, et al. Chitosan-silicate biocomposites to be used in modified drug release of 5-aminosalicylic acid (5-ASA). Appl Clay Sci. 2010;50:106–11. doi:10.1016/j.clay.2010.07.011.
3. Bayramoglu G, Senkal BF, Arica MY. Preparation of clay-poly(glycidyl methacrylate) composite support for immobilization of cellulase. Appl Clay Sci. 2013;85:88–95.
4. Zare Y, Garmabi H. Thickness, modulus and strength of interphase in clay/polymer nanocomposites. Appl Clay Sci. 2015;105–106:66–70.
5. Middea A, Fernandes TLAP, Neumann R, Gomes ODFM, Spinelli LS. Evaluation of Fe(III) adsorption onto palygorskite surfaces. Appl Surf Sci. 2013;282:253–8. doi:10.1016/j.apsusc.2013.05.113.
6. Rong J, Sheng MIA, Li H, Ruckenstein ELI. Polyethylene–palygorskite nanocomposite prepared via in situ coordinated polymerization. Polym Compos. 2002;2:658–65.
7. Ruiz-Hitzky E, Darder M, Fernandes FM, Wicklein B, Alcântara ACS, Aranda P. Fibrous clays based bionanocomposites. Prog Polym Sci. 2013;38:1392–414. doi:10.1016/j.progpolymsci.2013.05.004.
8. Shirvani M, Sherkat Z, Khalili B, Bakhtiary S. Sorption of Pb(II) on palygorskite and sepiolite in the presence of amino acids: equilibria and kinetics. Geoderma. 2015;249–250:21–7.
9. Wu J, Ding S, Chen J, Zhou S, Ding H. Preparation and drug release properties of chitosan/organomodified palygorskite microspheres. Int J Biol Macromol. 2014;68:107–12.
10. Peng Y, Chen D, Ji J, Kong Y, Wan H, Yao C. Chitosan-modified palygorskite: preparation, characterization and reactive dye removal. Appl Clay Sci. 2013;74:81–6. doi:10.1016/j.clay.2012.10.002.
11. Yu L, Gong J, Zeng C, Zhang L. Preparation of zeolite-A/chitosan hybrid composites and their bioactivities and antimicrobial activities. Mater Sci Eng C. 2013;33:3652–60.
12. Viseras MT, Aguzzi C, Cerezo P, Viseras C. Equilibrium and kinetics of 5-aminosalicylic acid adsorption by halloysite. Microporous Mesoporous Mater. 2008;108:112–6.
13. Rosa GS, Moraes MA, Pinto LAA. Moisture sorption properties of chitosan. LWT Food Sci Technol. 2010;43:415–20. doi:10.1016/j.lwt.2009.09.003.
14. Bergaya F, Theng BKG, Lagaly G. Handbook of clay science. 1st ed. Amsterdam: Elsevier; 2006.
15. Darder M, Ruiz-hitzky E. Biopolymer-clay nanocomposites based on chitosan intercalated in montmorillonite. Chem Mater. 2003;3774–80.
16. Wu J, Ding S, Chen J, Zhou S, Ding H. Preparation and drug release properties of chitosan/organomodified palygorskite microspheres. Int J Biol Macromol. 2014;68:107–12. doi:10.1016/j.ijbiomac.2014.04.030.
17. Auta M, Hameed BH. Modified mesoporous clay adsorbent for adsorption isotherm and kinetics of methylene blue. Chem Eng J. 2012;198–199:219–27. doi:10.1016/j.cej.2012.05.075.
18. An J-H, Dultz S. Polycation adsorption on montmorillonite: pH and T as decisive factors for the kinetics and mode of chitosan adsorption. Clay Miner. 2007;42:329–39.
19. Deng Y, Wang L, Hu X, Liu B, Wei Z, Yang S, et al. Highly efficient removal of tannic acid from aqueous solution by chitosan-coated attapulgite. Chem Eng J. 2012;181–182:300–6. doi:10.1016/j.cej.2011.11.082.
20. Rusmin R, Sarkar B, Liu Y, McClure S, Naidu R. Structural evolution of chitosan-palygorskite composites and removal of aqueous lead by composite beads. Appl Surf Sci. 2015;353:363–75. doi:10.1016/j.apsusc.2015.06.124.
21. Teixeira VG, Coutinho FMB, Gomes AS. Principais métodos de caracterização da porosidade de resinas à base de divinilbenzeno. Química Nova. 2001;24:808–18.
22. Celis R, Adelino MA, Hermosin MC, Cornejo J. Montmorillonite-chitosan bionanocomposites as adsorbents of the herbicide clopyralid in aqueous solution and soil/water suspensions. J Hazard Mater. 2012;209–210:67–76.
23. Jimenez RS, Maria S, Bosco D, Carvalho A. Remoção de metais pesados de efluentes aquosos pela zeólita natural escolecita-influência da temperatura e do pH na adsorção em sistemas monoelementares. Quim Nova. 2004;27:734–8.
24. Vanamudan A, Pamidimukkala P. Chitosan, nanoclay and chitosan-nanoclay composite as adsorbents for Rhodamine-6G and the resulting optical properties. Int J Biol Macromol. 2015;74:127–35. doi:10.1016/j.ijbiomac.2014.11.009.
25. De Gois Da Silva ML, Fortes AC, Oliveira MER, De Freitas RM, Da Silva Filho EC, De La Roca Soares MF, et al. Palygorskite organophilic for dermopharmaceutical application. J Therm Anal Calorim. 2014;115:2287–94.
26. Lin J, Zhan Y. Adsorption of humic acid from aqueous solution onto unmodified and surfactant-modified chitosan/zeolite composites. Chem Eng J. 2012;200–202:202–13. doi:10.1016/j.cej.2012.06.039.
27. Augsburger MS, Strasser E, Perinoa E, Mercaderb RC, Pedregosa JC. FTIR and MOSSBAUER investigation of a substituted palygorskite: silicate with a channel structure. J Phys Chem Solids. 1998;59:175–80.
28. Serna C, Vanscoyoc GE, Ahlrichs JL. Hydroxyl groups and water in palygorskite. 1977;62:784–92.
29. Suarez M, Garcia-Romero E. FTIR spectroscopic study of palygorskite: influence of the composition of the octahedral sheet. Appl Clay Sci. 2006;31:154–63.
30. Yan W, Liu D, Tan D, Yuan P, Chen M. FTIR spectroscopy study of the structure changes of palygorskite under heating. Spectrochim Acta A Mol Biomol Spectrosc. 2012;97:1052–7. doi:10.1016/j.saa.2012.07.085.
31. Oliveira MER, De Miranda Santos L, De Gois Da Silva ML, Da Cunha HN, Da Silva Filho EC, Da Silva Leite CM. Preparation and characterization of composite polyaniline/poly(vinyl alcohol)/palygorskite. J Therm Anal Calorim. 2015;119:37–46.
32. Mura C, Nácher A, Merino V, Merino-Sanjuán M, Manconi M, Loy G, et al. Design, characterization and in vitro evaluation of 5-aminosalicylic acid loaded N-succinyl-chitosan microparticles for colon specific delivery. Colloids Surf B Biointerfaces. 2012;94:199–205. doi:10.1016/j.colsurfb.2012.01.030.